Materials Science and Engineering A 402 (2005) 84–91

www.elsevier.com/locate/msea

# Freeform fabrication of titanium metal by 3D micro welding

M. Terakubo [a], Janghwan Oh [a], S. Kirihara [a], Y. Miyamoto [a,*], K. Matsuura [b], M. Kudoh [b]

[a] *Joining and Welding Research Institute, Smart Processing Research Center, Osaka University, Ibaraki, Osaka 567-0047, Japan*
[b] *Division of Materials Science and Engineering, Hokkaido University, Sapporo, Hokkaido 060-8628, Japan*

Received in revised form 31 March 2005; accepted 4 April 2005

**Abstract**

A novel freeform fabrication method named 3D micro welding (3DMW) has been developed. It is a combined process of the freeform fabrication method with TIG (tungsten inert gas) welding. The titanium micro beads were investigated with respect to the diameter, height, and contact angle to the titanium substrate as functions of arc discharge current and two different shielding gases. The Ar-4% $H_2$ gas was more effective in preventing oxidization of beads than Ar gas. Simple 3D titanium objects with arch, arabic numerals and pyramidal shapes were formed. Fine needle-like solidification structure of α-phase titanium were developed during bead formation due to the rapid cooling of the melt. The interfaces between a titanium bead and titanium substrate were jointed well without cracks or pores.


*Keywords:* Free form fabrication; 3D micro welding; Titanium; 3D objects

## 1. Introduction

Titanium has superior properties among metals such as high specific strength, chemical inertness, and low thermal conductivity. [1–5] However, its real application is still limited compared with other light metals, such as aluminum and magnesium, due to the high cost of raw materials and difficult processing. In order to overcome these shortcomings, several near net shape manufacturing techniques such as super plastic forming, isothermal forging, diffusion bonding, investment casting, and powder metallurgy have been developed. [6,7,8] While, various freeform fabrication methods such as laser cladding, droplet-based manufacturing (DBP), 3-D printing, shape deposition manufacturing (SDM), direct metal deposition (DMD), and 3-D welding have been attracted attention in recent years. [9–12] These methods enable the fabrication of custom objects with either soft (polymeric) or hard (steel or ceramic) materials directly from computer data of CAD/CAM system without using molds or dies. [13,14] Significant reductions in manufacturing costs and time to market production as well as savings of energy and materials are expected.

The use of welding technique to achieve the freeform fabrication was established in Germany in the 1960s and developed by many researchers. [15–17] However these 3-D welding techniques mainly focus on metals with low melting point, steel, and aluminium alloys in macro-scale.

We are developing a new freeform fabrication method named 3D micro welding (3DMW) to achieve freeforming of refractory metals and also intermetallics in micro-scale. In this technique, net shapes of refractory metals are formed directly from its thin metal wires. It is necessary, however for establishment of 3DMW to investigate the effects of controlling parameters such arc discharge current, shielding gas, thickness of metal wire, etc. on the object formation.

The aim of the present study is to optimize 3DMW process and demonstrate the capability of freeform fabrication of simple 3D titanium metal objects. Microstructure, hardness and composition of the objects formed by 3DMW were analyzed associated with the welding arc current and shielding gas.

## 2. Principle of 3D micro welding

The idea of 3DMW consists of a combination of two different techniques; freeform fabrication, also called rapid

* Corresponding author. Tel.: +81 6 6879 8693; fax: +81 6 6879 8693.
*E-mail address:* miyamoto@jwri.osaka-u.ac.jp (Y. Miyamoto).

0921-5093/$ – see front matter © 2005 Elsevier B.V. All rights reserved.
doi:10.1016/j.msea.2005.04.025

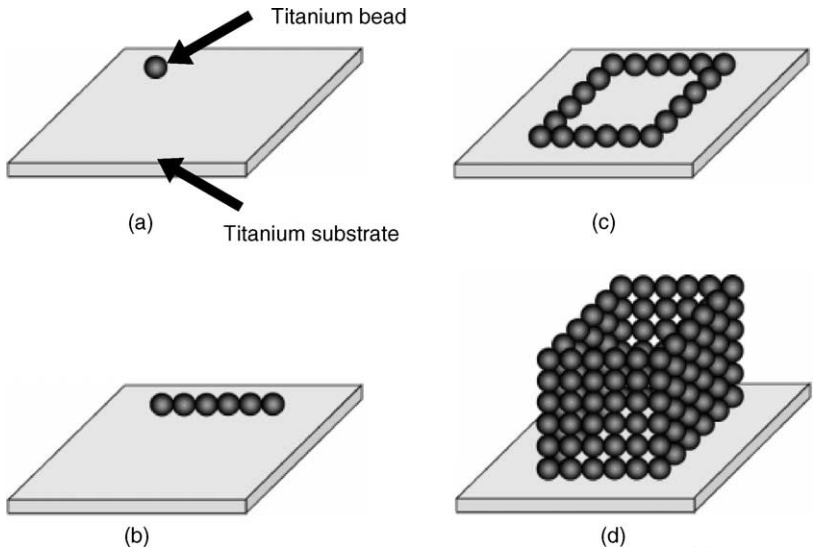


Fig. 1. Elemental process of 3D micro welding. (a) A titanium bead formation on the titanium substrate, (b) a 1D line object formation by titanium beads welding, (c) a 2D titanium object and (d) a 3D object of titanium.

prototyping, and TIG (tungsten inert gas) welding. The principle of 3DMW is shown in Fig. 1. A metal substrate is placed under the tungsten electrode for arc discharge. When pulsed micro-arcs are emitted, the tip of a thin metal wire with a diameter of 0.1–0.3 mm is fused and a micro metal bead is formed instantaneously. A fused bead is welded to a metal substrate or previously formed beads. By continuing this process and building up hot beads layer by layer under the control of CAD/CAM system, 3D metal objects can be produced. Fig. 2 shows photos of the 3DMW apparatus. It can be applied not only to titanium, but to other refractory metals such as tantalum, tungsten due to the high dense energy beam of the micro arc. When two different thin metal wires such as Ti and Ni, Ni and Al are fed alternately from the opposed spools, it is possible to built 3D complex structures and components composed of their alloys or intermetallic compounds.

## 3. Experimental procedure

The arc electrode used was a tungsten rod of 7 mm in length and 1 mm in diameter. The tip of the electrode was ground with a tip angle of 45°. The distance between the electrode and the substrate was adjusted to be 1.2 mm in this experiment. A titanium wire (99.6% purity, JIS 2-type, 200 μm in diameter) was fed automatically from a spool onto a titanium substrate (99.6% purity, JIS 1-type, 0.5 mm in thickness) by computer-controlled rotation of capstans. The

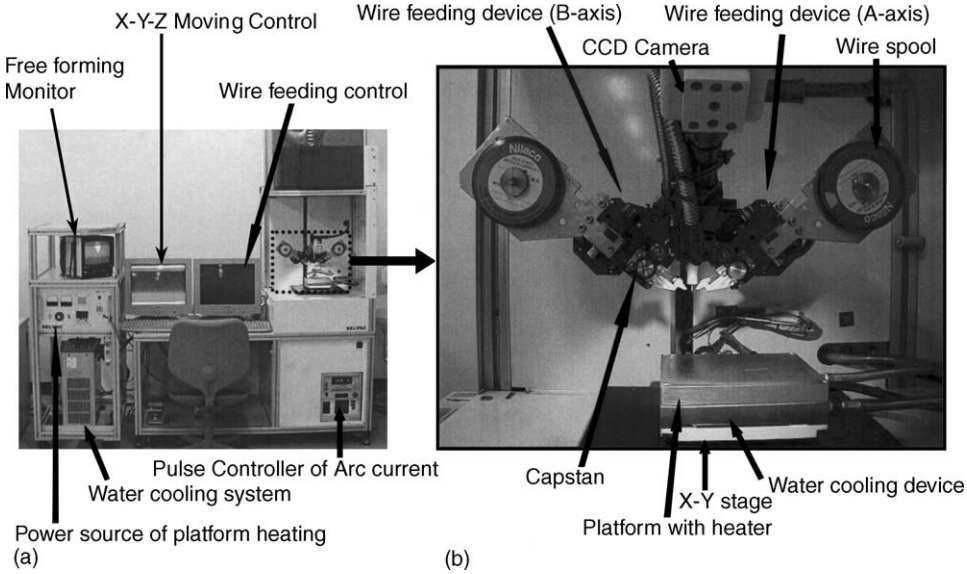


Fig. 2. (a) A 3DMW system and (b) freeforming station.

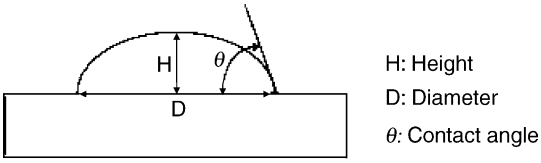


Fig. 3. Definitions of bead height, diameter and contact angle.

substrate was attached to the platform placed on a computer controlled X–Y stage and electrically grounded. The temperature of the platform could be raised to 300 °C using a built-in heating element and a water-cooling system. Pulsed arc current was discharged to the tip of wire and a micro bead of titanium was formed on the substrate. The pulsed current was controlled from 5A to 30A. Two different shielding gases of Ar and Ar-4%$H_2$ (forming gas), which flowed down around the electrode with the flowing rate of 2 l/min were tested for oxidization protection of metal beads. The wire feeding and the arc discharging motions were monitored by a CCD camera to check the formation of beads as shown in Fig. 2. The control program of wire feeding was installed on a computer. In this program, the feeding distance of a wire, which was from the tip of a wire to the programmed position for a bead formation on a substrate was measured on a computer and fed back for the next feeding of wire correctly.

The diameter and height of each bead formed and its contact angle to the substrate as shown in Fig. 3 were measured by using a magnifying projector. The bead positions formed were compared with the programmed positions to know the error range and probability of the bead formation.

The microstructures of the titanium beads formed were observed by using 3D-SEM. The cross section of a bead was observed by using an optical microscope. The chemical composition at the bead joint was analyzed by means of X-ray microanalysis. The hardness measurement on the cross section of a titanium bead and object was carried out by using a Vickers hardness tester.

## 4. Results and discussion

In the formation of titanium beads by 3DMW, the size, shape and microstructure depend on the arc peak current and shielding gas. Fig. 4 shows titanium beads formed under two different shielding gas flows as a function of the arc peak current. An oxidized area was observed in dark green and deep blue colors around each titanium bead welded on the titanium substrate. It increased from 1.1 to 3.3 mm as the arc peak current increased from 5A to 30A when Ar gas was used for shielding gas (Fig. 4(a), (b) and (c)). However, such oxidization was remarkably reduced as an Ar-4%$H_2$ gas was used (Fig. 4(d), (e) and (f)).

Fig. 5 shows the diameter, height and contact angle of these titanium beads. As the arc peak current increased from 5A to 30A, the height and the contact angle were decreased. But the bead diameter increased from 0.5 to 0.8 mm under

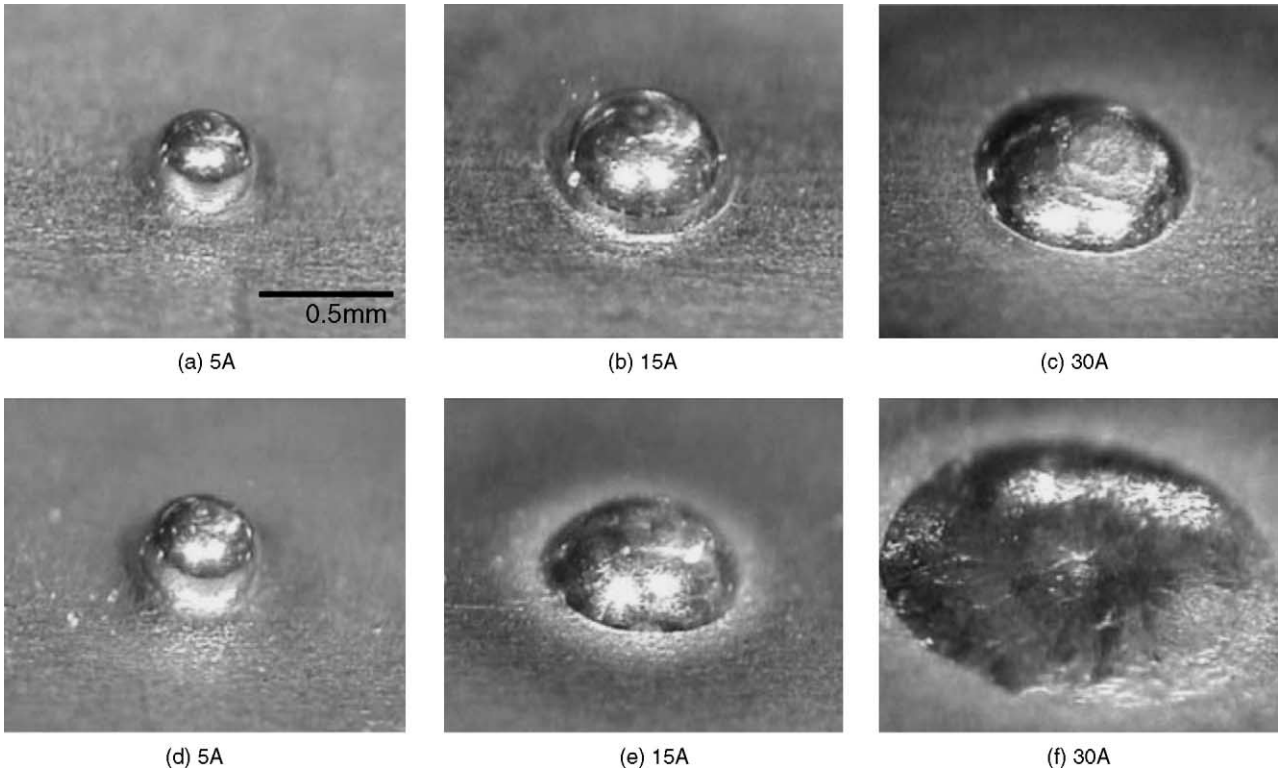


Fig. 4. Photo images of titanium beads made by each arc current under Ar ((a), (b) and (c)) and Ar-4%$H_2$ ((d), (e) and (f)) gases.

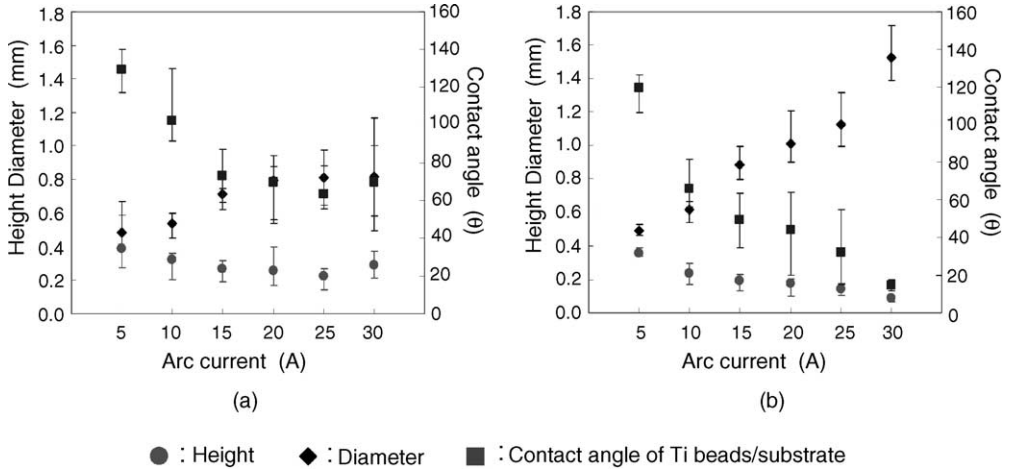


Fig. 5. Geometry and contact angle of titanium beads formed under (a) Ar gas and (b) Ar-4%$H_2$ gas as a function of arc current.

an Ar gas flow, while it further increased to 1.5 mm under an Ar-4%$H_2$ gas.

Fig. 6(a), (b) and (c) show the microstructure of a titanium bead formed on the titanium substrate at 20A under an Ar gas flow. The joint interface is indicated with a white line. Needle–like microstructure was developed in the bead. This microstructure was thought to be dendrites of α-phase titanium, which was formed by rapid cooling of a molten bead. Vickers hardness measured on the cross section of a bead formed on the substrate was 2.6 GPa at the joint interface, and 4.3 GPa at the central part of a bead. Fig. 6(d), (e) and (f) show the microstructure of a titanium bead formed under an Ar-4%$H_2$ gas flow. The titanium bead penetrated into the substrate suggesting a higher heat transfer to the bead and substrate compared with the use of Ar gas. The hardness at the joint interface was 1.7 and 3.3 GPa at the central part of a bead. Vickers hardness of the titanium substrate itself was 1.2 GPa. The influence of oxidization may give higher hardness of titanium beads formed under Ar gas flow. Although some micro pores (5–10 μm) were found near the joint interface, there was no crack or large pore.

Fig. 7 shows the beads, which were formed automatically at checkered positions by CAD/CAM system. Addition of 4% $H_2$ to Ar gas influenced largely to the size and shape of beads. Fig. 8 shows the height and diameter of these titanium beads, and the deviation from programmed positions. When the beads formed under an Ar gas flow (Fig. 8(a)), the mean height and diameter were quite uniform, 0.26 and 0.71 mm, respectively. The mean deviation from programmed positions on *x*-axis was −0.17 mm and on *y*-axis was +0.03 mm. Thus, the deviation from *x*-axis was larger than that from *y*-axis. When the beads were formed under an Ar-4%$H_2$ gas flow (Fig. 8(b)), the mean height was 0.18 mm and the mean diameter was 0.9 mm, but a little scattered. The mean deviation

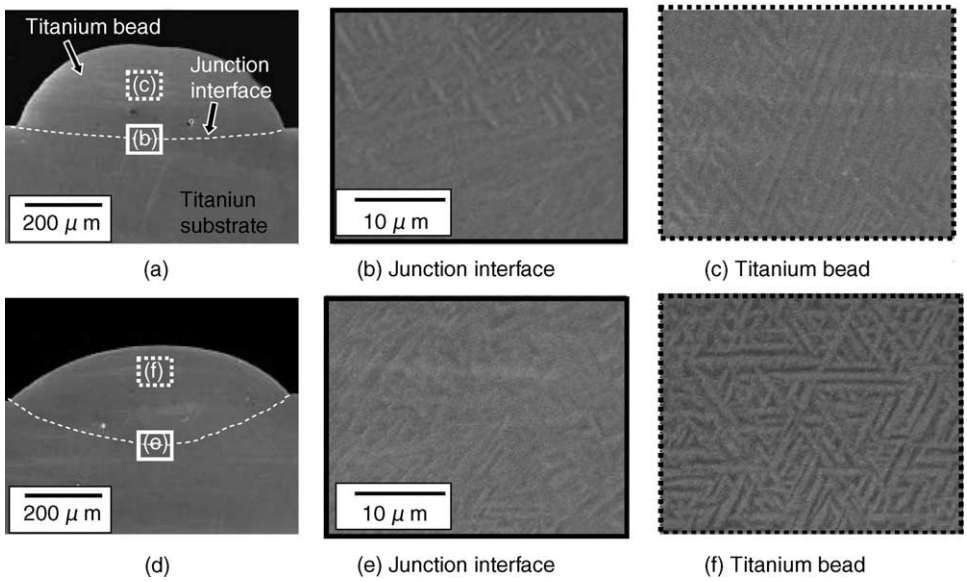


Fig. 6. SEM images of a titanium bead formed under Ar ((a), (b) and (c)) and Ar-4%$H_2$ ((d), (e) and (f)) gases.

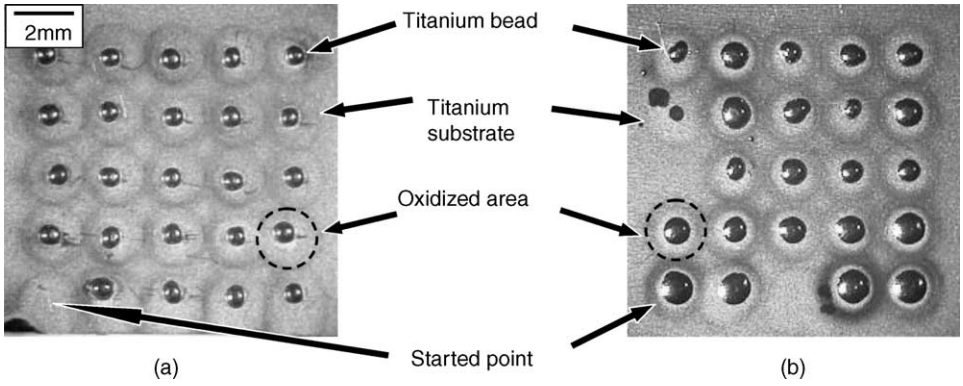


Fig. 7. Grid patterns of titanium beads formed by auto-program under (a) Ar gas and (b) Ar-4%$H_2$ gas.

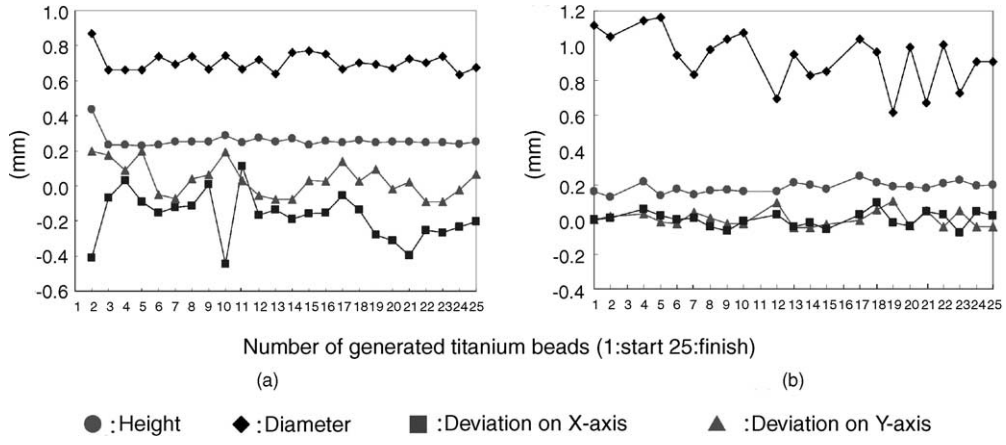


Fig. 8. Dispersion of titanium beads size and deviation of bead position: (a) under Ar gas and (b) under Ar-4%$H_2$ gas.

from programmed positions on *x*-axis was +0.02 mm and that on *y*-axis was −0.05 mm. The *x*-axis deviation of titanium beads formed under an Ar-4%$H_2$ gas flow was much smaller than that formed under an Ar gas flow. Just after the pulsed micro-arc was emitted, a small molten pool due to high temperature of arc was formed at programmed position of the substrate surface. [18,19] Even if the position of a bead was slightly shifted from the programmed position, the molten bead was thought to be poured into the pool. This effect can act to reduce the deviation of bead position from the programmed position. Comparing to the use of Ar gas, the frequency in formation of a molten pool was much higher under Ar-4%$H_2$ gas flow.

Fig. 9 shows nine standing pin objects of titanium. Thirty titanium beads were stacked on a fixed *z*-axis by successive micro-arc discharging and a single titanium pin was built, where samples (a) and (b) were prepared under the Ar gas and the Ar-4%$H_2$ gas, respectively. Fig. 10 shows the diam-

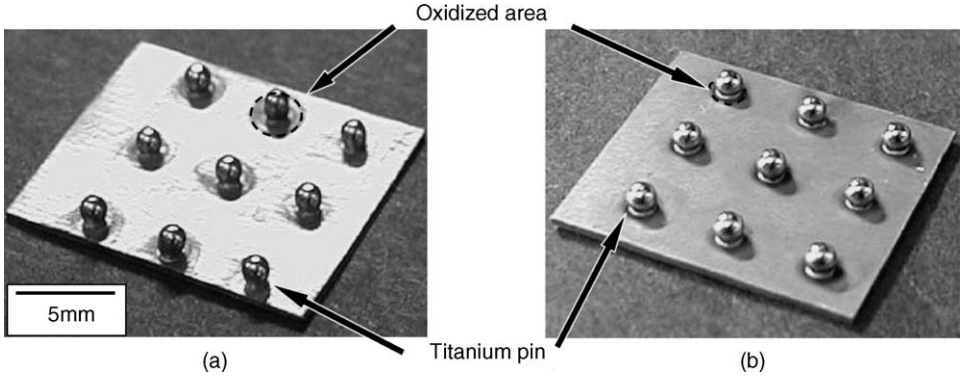


Fig. 9. Feature of titanium pin objects. Grid pattern of nine titanium pins formed under (a) Ar gas and (b) Ar-4%$H_2$ gas.

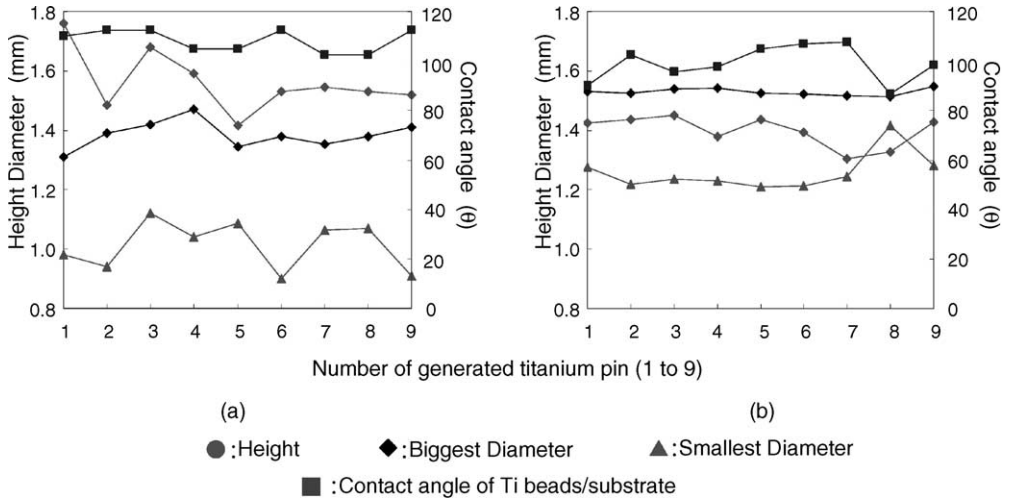


Fig. 10. Geometry and contact angle of titanium pins formed under (a) Ar gas and (b) Ar-4%$H_2$ gas.

eter, height and contact angle of each pin. When the pins were formed under an Ar gas, the diameter ranged from 1.02 to 1.38 mm. Mean height and contact angle of each pin were 1.56 mm and 109°, respectively. However, when they were formed under Ar-4%$H_2$ gas, the diameter expanded to 1.26–1.53 mm. And the mean height and contact angle were 1.40 mm and 98°, respectively. The mean thickness of one layer was calculated to be 52 μm when formed under Ar gas, and 47 μm under Ar-4%$H_2$ gas. High heat transfer of the Ar-4%$H_2$ gas might form thicker titanium pins, but thin bead layers as shown in Fig. 4. [20].

The microstructure of titanium pin objects formed under Ar gas and Ar-4%$H_2$ gas are shown in Fig. 11. There was no crack or pore at the joint interface in both pins. The welding between beads was successful. Both microstructures were quite homogeneous. These results suggest that the titanium wire was entirely melted and welded by the micro-arc. As shown in Fig. 6, fine needle-like dentritic microstructure of α-phase titanium were formed in a titanium pin object.

Vickers Hardness profile across a titanium pin object from the bottom to top is shown in Fig. 12. In both cases of titanium pin formation under the Ar gas and the Ar-4%$H_2$ gas, the hardness showed the broad maxima at the distance in the range of 200–500 μm from the substrate. There were some pores, 1–5 μm in diameter near the top part of a pin. But no pore was found at the center. When molten titanium beads were dropped on the top of a titanium pin object, the entrapped gas should form pores near the bead surface.

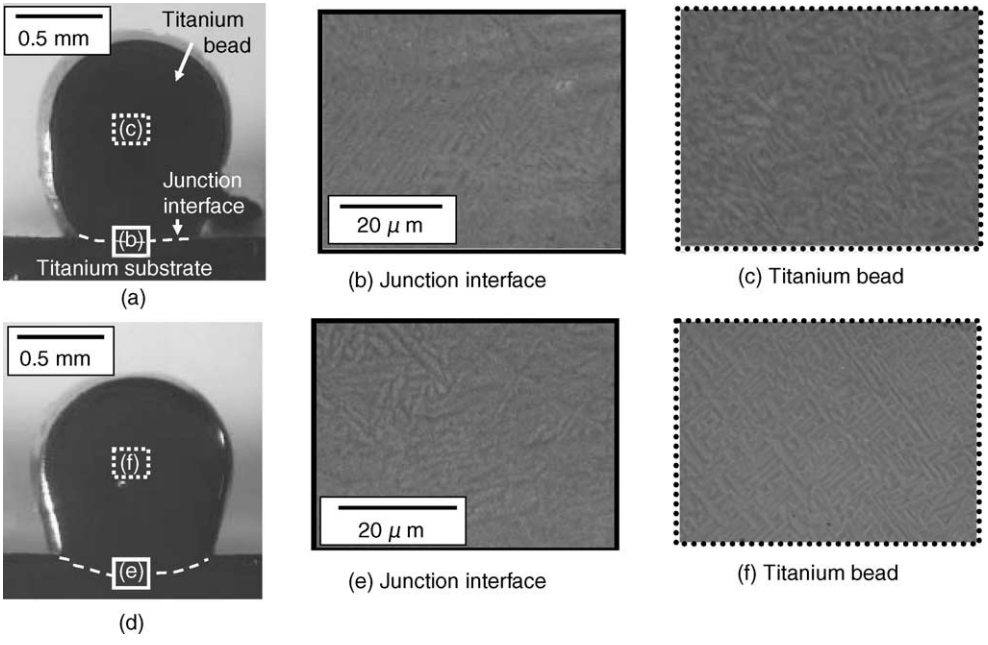


Fig. 11. OM and SEM images of a titanium pin object under Ar ((a), (b) and (c)) and Ar-4%$H_2$ ((d), (e) and (f)) gases.

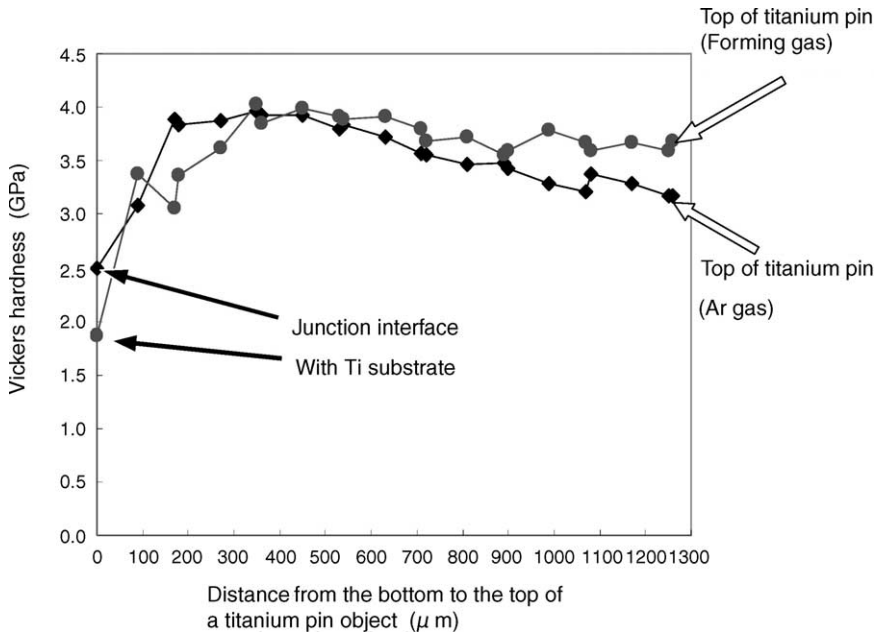


Fig. 12. Vickers hardness profile of a titanium pin object.

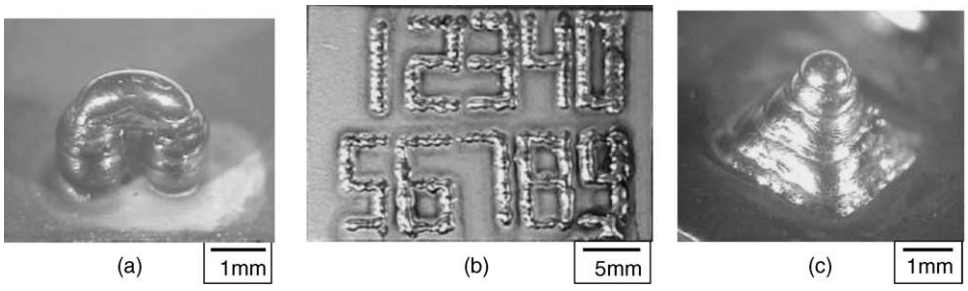


Fig. 13. Photo images of titanium objects formed. (a) An arch shape, (b) Numbers and (c) A titanium pyramid.

[21,22] However, such pores may disappear by re-melting due to successive arc-discharge and stacking of molten beads. It is considered, therefore, that the pin formation may always produce pores near the top leaving behind the dense structure, resulting in the hardness profile with a broad maximum as shown in Fig. 12.

Fig. 13 shows some simple 3D titanium objects, which were formed by continuous stacking and welding of a titanium bead. Fig. 13(a) is an arch-shaped object. This was formed by bridging two titanium pins of 30 layers. Fig. 13(b) shows titanium numbers formed of about 250 titanium beads. Fig. 13(c) is a small titanium pyramid, which was formed by decreasing the pulsed current from 30A to 10A from the bottom to the top layer.

## 5. Conclusions

A novel freeform fabrication method named 3D micro welding (3DMW) has been developed using an idea to combine freeform fabrication method with TIG (tungsten inert gas) welding. The optimization of forming parameters, such as arc current, bead diameter and contact angle were investigated. As the arc current increased, the height and the contact angle of titanium beads were decreased, but the diameter increased. Two kinds of shielding gas (Ar gas and Ar-4%$H_2$ gas) were compared, and the Ar-4%$H_2$ gas was found to be more useful to prevent oxidization of beads. The titanium bead formed showed fine needle-like dentritic microstructure of α-phase titanium during bead formation due to the rapid cooling. Simple 3D titanium objects were formed by continuous stacking and welding of titanium beads under computer control. There are some pores in a titanium bead and an object, but the interface between beads or bead and substrate were jointed well without cracking.

## References

[1] CRC Materials Science and Engineerig Hand book, p. 46.
[2] M. Hoffman, E. Vosges, J. Micromech. Microeng. 12 (2002) 438–443.
[3] C. Choi, H.T. Kim, Y.T. Lee, Y.W. Kim, C.S. Lee, Mater. Sci. Eng. A 329 (2002) 545–556.

[4] D.B. Lee, K.B. Park, J.W. Jeong, S.E. Kim, Mater. Sci. Eng. A 328 (2002) 161–168.
[5] S.E. Kim, Y.T. Lee, M.H. Oh, H. Inui, M. Yamaguchi, Mater. Sci. Eng. A 329 (2002) 25–30.
[6] Masuo Hagiwara, Satoshi Emura, Mater. Sci. Eng. A 352 (2003) 85–92.
[7] F.H. Froes, D. Eylon, Int. Master. Rev. 35 (1990) 161–182.
[8] S. Das, J. Josepin, Beaman, M. Wohlert, L. David, Bourell, Rapid Prototyping J. 4 (1998) 112–117.
[9] E.W. Kreutz, G. Backes, A. Gasser, K. Wissenbach, Appl. Surf. Sci. 86 (1995) 310.
[10] G.K. Lewis, Mater. Technol. 10 (3-4) (1995) 51.
[11] X. Yan, P. Gu, Comput. Aided Des. 28 (1996) 307.
[12] J.H. Chun, C.H. Passow, CIRP Ann. 42 (1993) 235.
[13] M.K. Agarwala, A. Bandyopadhyay, R. van Weeren, V. Jamalabad, P. Whalen, N.A. Langrana, A. Safari, S.C. Danforth, J. Rapid Prototyping 2 (1996) 4–19.
[14] M.K. Agarwala, A. Bandyopadhyay, R. van Weeren, V. Jamalabad, P. Whalen, N.A. Langrana, S.C. Danforth, A. Safari, Bull. Am. Cer. Soc. 75 (1996) 60–65.
[15] D.S. Choi, S.H. Lee, B.S. Shin, J. Mater. Process. Technol. 113 (2001) 273–279.
[16] Y.M. Zhang, P. Li, Y. Chen, A.T. Male, Mechatronics 12 (2002) 37–53.
[17] H. Wang, R. Kovacevic, J. Eng. Manuf. 215 (2001) 1519–1527.
[18] D.L. Poprovka, L.P. Moisov, Metal Sci. Heat Treat. 44 (2002) 462–463.
[19] H.G. Fan, R. Kovacevic, Metall. Mater. Trans. B 3 (1999) 791.
[20] P. Fauchais, M. Vardelle, Pure Appl. Chem. 66 (1994) 1247–1258.
[21] L. Liu, G. Song, G. Liang, J. Wang, Mater. Sci. Eng. A 390 (1–2, 15) (2005) 76–80.
[22] J. Oh, N. Kim, S. Lee, E. Lee, Mater. Sci. Eng. A 340 (1–2, 15) (2003) 232–242.